

# Chemical lithiation induced $\text{Li}_{4.4}\text{Sn}$ lithiophilic layer for Anode-free Lithium Metal Batteries

Zibo Zhang<sup>a,b</sup>, Hao Luo<sup>a</sup>, Zhenyuan Liu<sup>a,b</sup>, Shuhui Wang<sup>a,b</sup>, Xufeng Zhou<sup>a,\*</sup>, Zhaoping Liu<sup>a,\*</sup>

<sup>a</sup> Advanced Li-ion Battery Engineering Laboratory, CAS Engineering Laboratory for Graphene and Key Laboratory of Graphene Technologies and Applications of Zhejiang Province, Ningbo Institute of Materials Technology and Engineering (NIMTE), Chinese Academy of Sciences, Ningbo 31520, P. R. China

<sup>b</sup> College of Materials Science and Opto-Electronic Technology, University of Chinese Academy of Sciences (UCAS), Beijing 100049, P. R. China

✉ Corresponding author. E-mail: [liuzp@nimte.ac.cn](mailto:liuzp@nimte.ac.cn) (Z. Liu); [zhouxf@nimte.ac.cn](mailto:zhouxf@nimte.ac.cn) (X. Zhou)

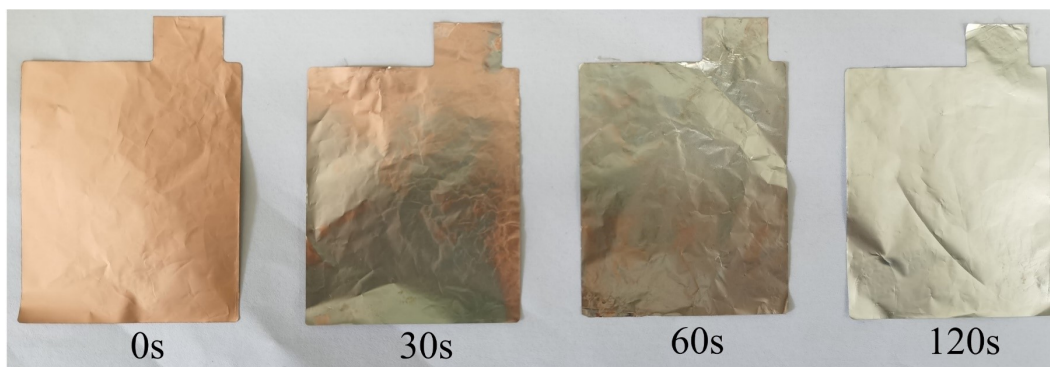


**Figure S1.** Optical image of Sn@Cu electrode with different processing time.

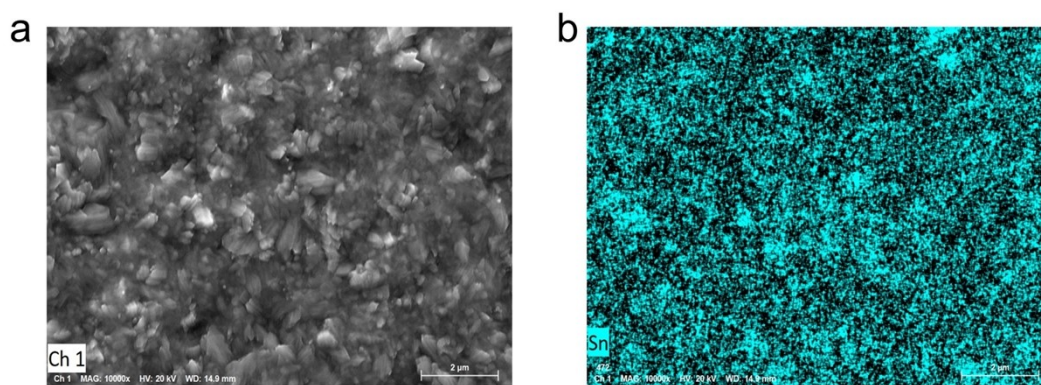


**Figure S2.** a) Top-view SEM image and b) elemental mapping of of Sn@Cu.

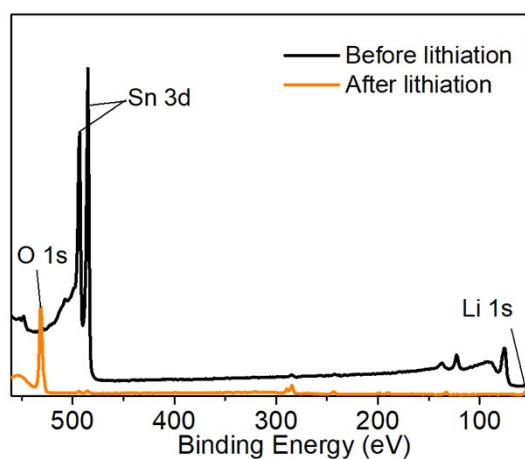


Figure S3. XPS spectra of Sn@Cu foil before and after lithiation.

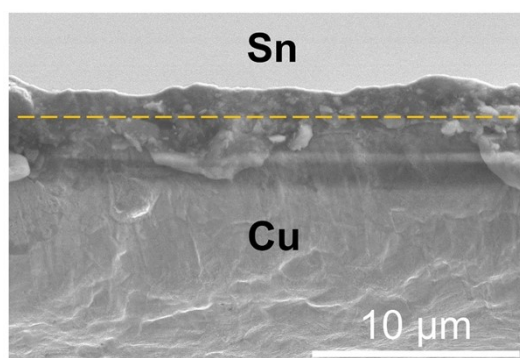
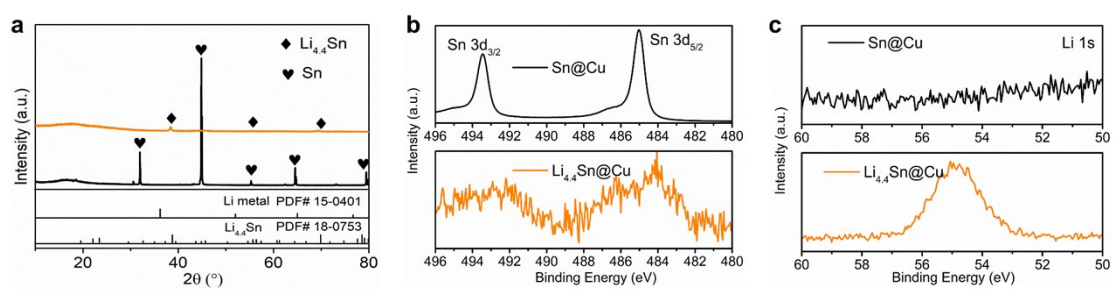
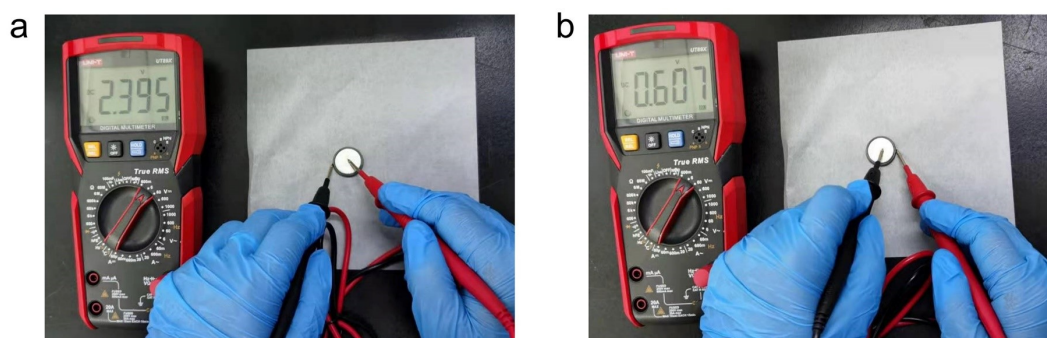


Figure S4. Cross-sectional SEM image of Sn@Cu before lithiation.



**Figure S5.**a) XRD patterns of  $\text{Li}_{4.4}\text{Sn@Cu}$  and  $\text{Sn@Cu}$ . b) Sn 3d XPS spectra of  $\text{Sn@Cu}$  (up) and  $\text{Li}_{4.4}\text{Sn@Cu}$  (down) electrodes. c) Li 1s XPS spectra of  $\text{Sn@Cu}$  (up) and  $\text{Li}_{4.4}\text{Sn@Cu}$  (down).



**Figure S6.** Measurement of open circuit voltage of a)  $\text{Li}_{4.4}\text{Sn@Cu}$  / NCM811 cell and b)  $\text{Cu}$  / NCM811 cell.

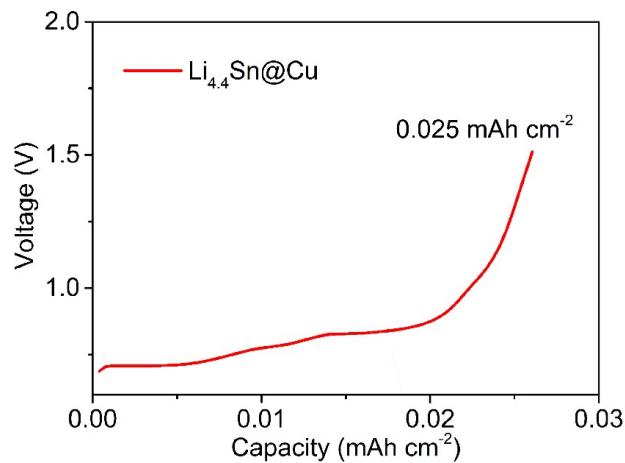


**Figure S7.** Measurement of lithium inventory of  $\text{Li}_{4.4}\text{Sn@Cu}$  electrode.

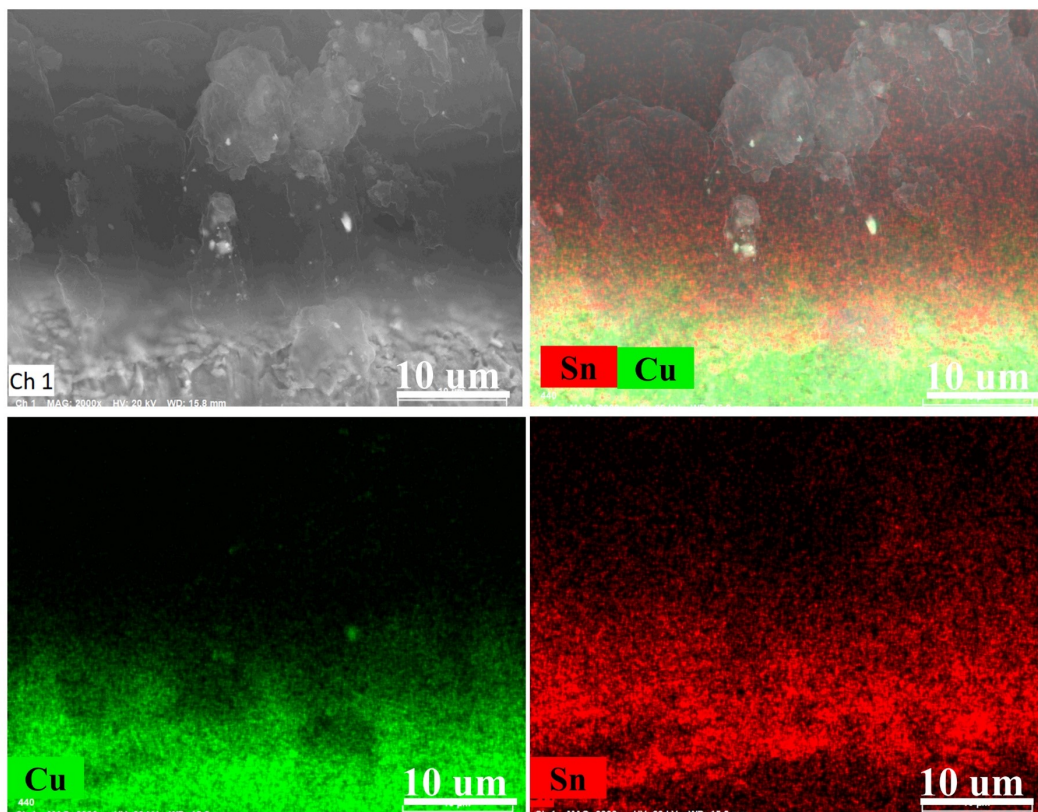


**Figure S8.** a) Cross-sectional SEM image of  $\text{Li}_{4.4}\text{Sn@Cu}$  electrode after 3  $\text{mAh cm}^{-2}$  Li plating with a current density of 0.5  $\text{mA cm}^{-2}$ , and b-d) the corresponding EDS mapping.



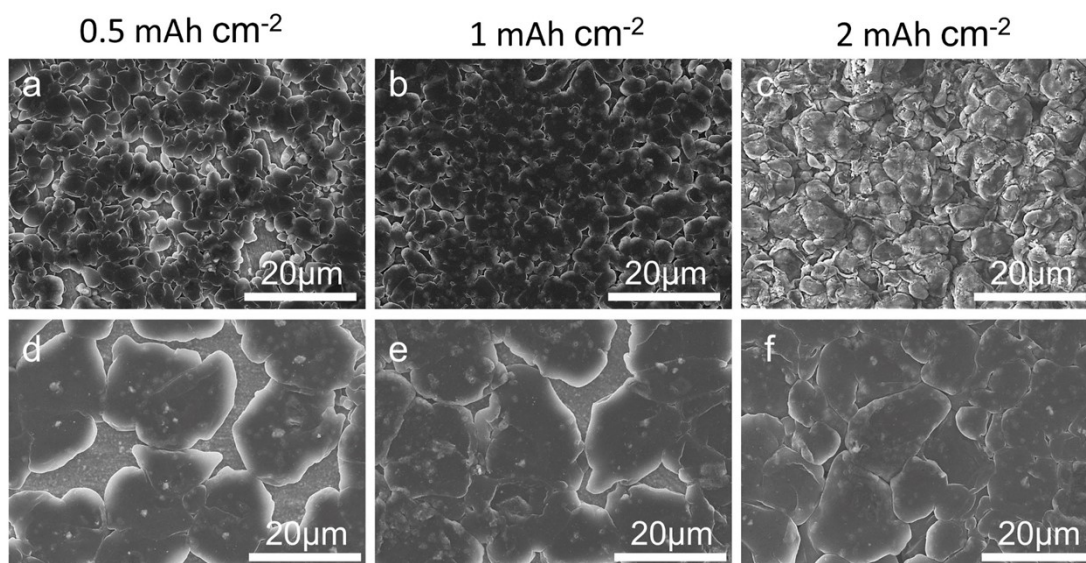


**Figure S9.** Surface morphology of Cu and  $\text{Li}_{4.4}\text{Sn}@\text{Cu}$ . a-c) Top-view SEM images of Cu after Li deposition with different areal capacities. d-f) Top-view SEM images of  $\text{Li}_{4.4}\text{Sn}@\text{Cu}$  after Li deposition with different areal capacities.

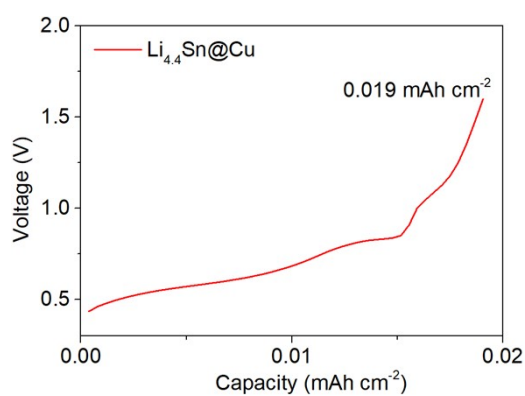


**Figure S10.** Lithium inventories of  $\text{Li}_{4.4}\text{Sn}@\text{Cu}$  electrodes after the first cycle measured by galvanostatic charging.

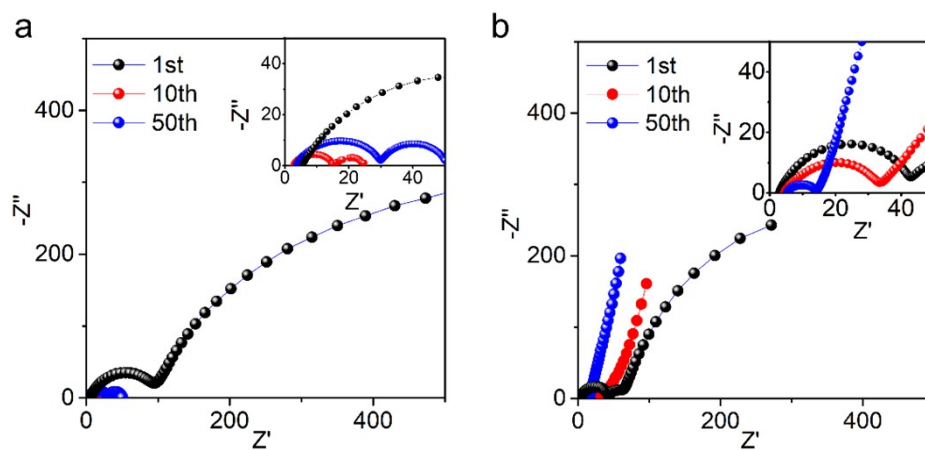


**Figure S11.** EIS analysis of the resistance evolution during cycling in half cells with Cu and  $\text{Li}_{4.4}\text{Sn}@\text{Cu}$  electrode.

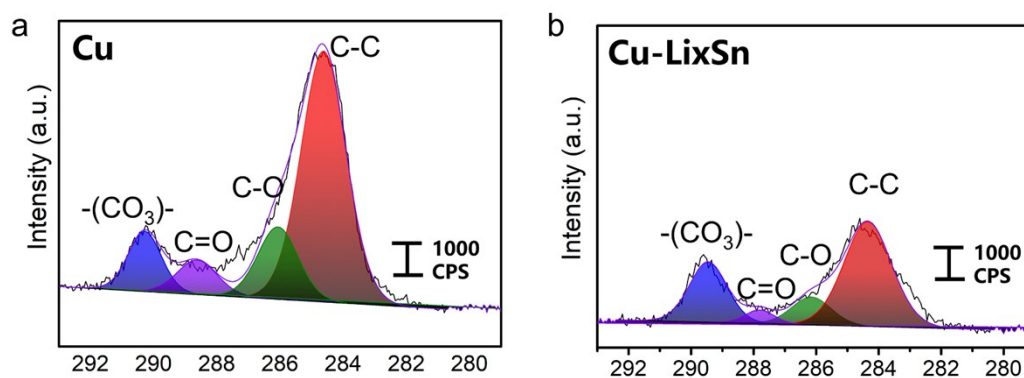


**Figure S12.** C 1s XPS spectra of a) Cu and b)  $\text{Li}_{4.4}\text{Sn}@\text{Cu}$  electrodes obtained from the cells after 10 cycles.

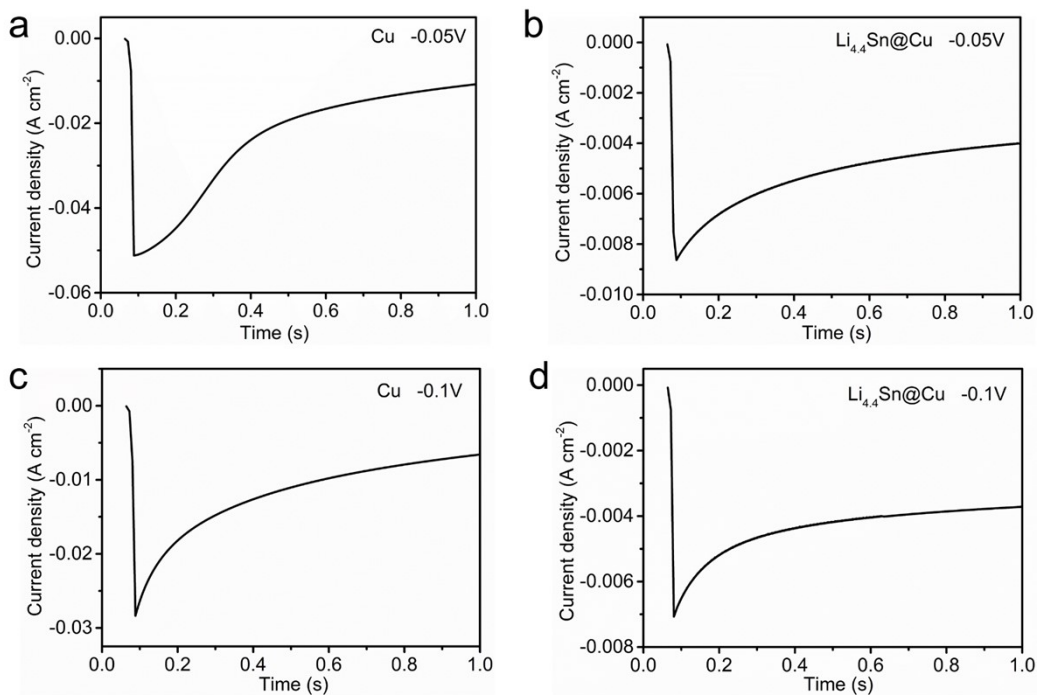


**Figure S13.** Current transients of Li deposition on different substrates at different potential. a, c) Cu. b, d)  $\text{Li}_{4.4}\text{Sn}@\text{Cu}$ .

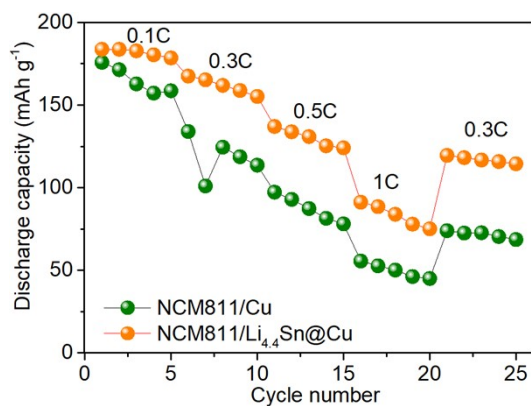


**Figure S14.** The rate performance of  $\text{Li}_{4.4}\text{Sn}@\text{Cu}/\text{NCM811}$  and  $\text{Cu}/\text{NCM811}$  full cells.



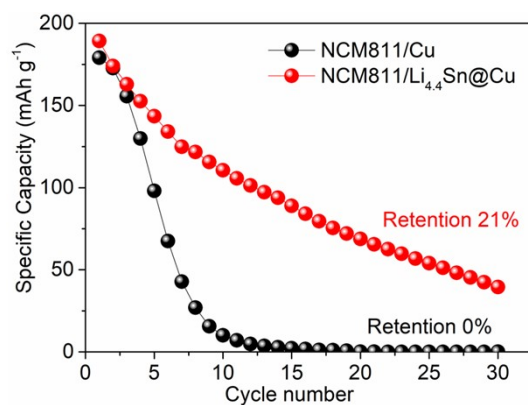


**Figure S15.** Cycling performance of NCM811/Cu and NCM811/Li<sub>4.4</sub>Sn@Cu cells in carbonate-based electrolyte.

**Table S1.** The comparison on parameters of anode free coin cells in this work and previously reported works.

	Areal capacity (mAh cm <sup>-2</sup> )	Voltage (V)	Current density (mA)	Cycle number	Capacity retention (%)
This work	4	4.3	0.6	50	85.5
[18]	2.6	3.8	0.9	60	70
[22]	2	4.3	0.2	50	40
[27]	2	3.8	0.2	50	65
[29]	0.765	3.8	0.15	50	74
[35]	1.6	4.3	0.2	20	48
[36]	1.5	4	0.5	60	53
[37]	2.2	4.5	0.5	60	55.7

As the data of pouch-cell AFLMB related to current collector modification have rarely been reported, only comparisons of coin-type cell data were performed. It shows that our cell exhibits better overall performance, especially in high-capacity load cathode and cycle life.

- [18] Chen W, Salvatierra R V, Ren M, et al. *Adv Mater.* **2020**, 2002850
- [22] T.T. Hagos, B. Thirumalraj, C.J. Huang, L.H. Abrha, T.M. Hagos, G.B. Berhe, H.K. Bezabh, J. Cherng, S.F. Chiu, W.N. Su, B.J. Hwang, *ACS Appl Mater Inter*, 11 (2019) 9955-9963.
- [27] A.A. Assegie, C.C. Chung, M.C. Tsai, W.N. Su, C.W. Chen, B.J. Hwang, *Nanoscale*, 11 (2019) 2710-2720.
- [29] A.A. Assegie, J.H. Cheng, L.M. Kuo, W.N. Su, B.J. Hwang, *Nanoscale*, 10 (2018) 6125-6138.
- [35] T.M. Hagos, G.B. Berhe, T.T. Hagos, H.K. Bezabh, L.H. Abrha, T.T. Beyene, C.-J. Huang, Y.-W. Yang, W.-N. Su, H. Dai, B.-J. Hwang, *Electrochim. Acta*, 316 (2019) 52-59.
- [36] H. Liu, X. Yue, X. Xing, Q. Yan, J. Huang, V. Petrova, H. Zhou, P. Liu, A scalable 3D lithium metal anode, *Energy Storage Mater.* 16 (2019) 505-511.
- [37] Z.T. Wondimkun, W.A. Tegegne, J. Shi-Kai, C.-J. Huang, N.A. Sahalie, M.A. Weret, J.-Y. Hsu, P.-L. Hsieh, Y.-S. Huang, S.-H. Wu, W.-N. Su, B.J. Hwang, *Energy Storage Materials.* 35 (2021) 334-344.